CHEMICAL ENGINEERING TRANSACTIONS
VOL. 27, 2012
Guest Editors: Enrico Bardone, Alberto Brucato, Tajalli Keshavarz

ISBN 978-88-95608-18-1; **ISSN** 1974-9791

A publication of AIDIC
The Italian Association of Chemical Engineering
Online at: www.aidic.it/cet

DOI: 10.3303/CET1227039

Large-scale Radiation Manufacturing of Hierarchically Assembled Nanogels

Clelia Dispenza*[a,b], Maria Antonietta Sabatino[a], Natascia Grimaldi[a], Giuseppe Spadaro[a], Donatella Bulone[b], Maria Luisa Bondì[c], Giorgia Adamo[d], Salvatrice Rigogliuso[d]

[a]Dipartimento di Ingegneria Chimica, Gestionale, Informatica, Meccanica, Università degli Studi di Palermo, Edificio 6, Viale delle Scienze 90128 Palermo, Italy
[b]CNR-Istituto di Biofisica U:O.S. di Palermo, via Ugo La Malfa 153 90146 Palermo, Italy
[c]CNR-Istituto per lo Studio dei Materiali Nanostrutturati (ISMN), via Ugo La Malfa, 153 90146 Palermo, Italy
[d]Dipartimento di Scienze e Tecnologie Molecolari e Biomolecolari, Università degli studi di Palermo, Viale delle Scienze, Edificio 16, 90128 Palermo, Italy
clelia.dispenza@unipa.it

Nanogels (NGs), or small particles formed by physically or chemically crosslinked polymer networks, represent a niche in the development of “smart” nanoparticles for drug delivery and diagnostics. They offer unique advantages over other systems, including a large and flexible surface for multivalent bio-conjugation; an internal 3D aqueous environment for incorporation and protection of (bio)molecular drugs; the possibility to entrap active metal or mineral cores for imaging or phototherapeutic purposes; stimuli-responsiveness to achieve temporal and/or site control of the release function and biocompatibility. The availability of inexpensive and robust preparation methodologies is at the basis of the development of effective nanogel-based theragnostic devices. The design rules for mass fabrication of nanoscale hydrogel particles with the recourse to industrial-type accelerators is here discussed.

1. Introduction

Nanogels are particles formed by physically or chemically crosslinked polymer networks of nanoscalar size. They are very promising carriers for drug delivery and have some favorable properties, such as high biocompatibility, a large surface area for bioconjugation and an internal 3D aqueous network for the incorporation of bioactive molecules, inorganic nanocrystals or magnetic nanoparticles useful as contrast agents for optical and magnetic imaging. The smooth and elastic outlayers make these nanoparticles able to penetrate through small pores and channels and generate extremely low friction with various biological surfaces. Their tunable size and chemical functionalities enable NGs responsiveness to environmental factors and biodegradability, when required. The design of functional nanoparticles must include a high degree of control of product properties through both process and material chemistry.
Major synthetic strategies for the preparation of nanogels belong to either micro-fabrication methodologies (photolithography, microfluidic, micromoulding) or to self-assembly approaches that exploit ionic, hydrophobic or covalent interactions (Oh et al., 2008, Morimoto et al., 2005, Gonçalves et al., 2010 and reference herein). For the latter, in particular, dimensional control

Please cite this article as: Dispenza C., Sabatino M.A., Grimaldi N., Spadaro G., Bulone D., Bondi M.L., Adamo G. and Rigogliuso S., 2012, Large-scale radiation manufacturing of hierarchically assembled nanogels, Chemical Engineering Transactions, 27, 229-234 DOI: 10.3303/CET1227039

has been often achieved by the recourse to surfactants. Therefore, while micro-fabrication methods are limited by the need of costly equipments, the recourse to surfactants as well as organic solvents, initiators and catalysts may detrimentally affect the toxicological profile of the nanogels produced in colloidal systems. The availability of inexpensive and robust preparation methodologies is at the basis of the development of effective nanogel-based theragnostic devices. Radiation induced cross-linking is a versatile and "clean" process, it generally yields highly pure materials through environmentally friendly and economically viable processes (Rosiak and Olejniczak, 1993; Rosiak et al., 1995; Rosiak and Yoshii,1999; Lugao and Malmonge, 2001; Peppas et al., 2006). High energy radiation processing demonstrated its potential for the production of nanogels already in the late '90s, owing to the pioneeristic work of Rosiak and collaborators, but since then no adequate efforts have been spent in developing a viable technology based on these findings to generate multi-functional nanoparticles with the required properties (Ulanski, et al.,1998). This paper documents the potential of e-beam irradiation to generate consistently and quantitatively biocompatible base and amino-functionalised poly(N-vinyl-pyrrolidone) (PVP) nanogel variants, as for dimensions and chemical structure, and thereby functionality, from the aqueous solutions of their polymer and monomer precursors.

2. Experimental

PVP k60 (Aldrich, Mn=1.60 x 105 g/mol, Mw = 4.1 x 105 g/mol, Rg = 27 nm (Dispenza et al., 2011)) and (3-aminopropyl)methacrylamide hydrochloride (APMAM, Polyscience) were used as received. PVP aqueous solutions at different polymer concentration (from 10 % to 0.05 %wt) were carefully deoxygenated with gaseous nitrogen. PVP aqueous solutions at 0.1 %wt were added with APMAM, the primary amino groups carrying monomer, at different concentrations (1:200, 1:100 and 1:50 molar ratios with respect to PVP RU). Electron beam irradiation was performed using two 10 MeV linear accelerators at the ICHTJ of Warsaw (Poland): LAE 13/9, which allowed to select two different average dose-rates, by tuning pulse repetition rate and duration time (100 kGy/h, 500 kGy/h), and many different doses by varying the irradiation time; Electronika, that is equipped with a conveyor belt that allows many vials in a tray to pass under the beam at a given speed, which was set to supply 40 kGy per pass. In this last condition a much higher average dose-rate was achieved. Temperature was always maintained between 4-10 °C. Macroscopically gelled systems obtained at the higher polymer concentrations in the investigated range were separated from their soluble portions and successively freeze-dried. Nanogel dispersions obtained at 0.5, 0.25, 0.1 and 0.05 %wt were dialyzed against distilled water for 48 h using dialysis tubes of 12-100 kDa cut-off (Aldrich). The yield of the process was determined gravimetrically. Molecular structure of the macro/nanogels produced was confirmed trough FT-IR and solid-state ^{13}C-NMR. FTIR analysis was carried out with Perkin Elmer-Spectrum 400 apparatus by dispersing the freeze-dried residues in potassium bromide and compressing into pellets. Spectra were recorded at 30 scans per spectrum and 1 cm^{-1} resolution in the 4000-400 cm^{-1} range. The average hydrodynamic diameter, Dh, and the relative standard deviation (giving information on the width of the particle size distribution) were measured by dynamic light scattering (DLS), using a Brookhaven Instruments BI200-SM goniometer. Samples were kept at constant temperature of 20±0.1 °C. The light scattered intensity and time autocorrelation function were measured by using a Brookhaven BI-9000 correlator and a 100 mW Ar laser (Melles Griot) tuned at λ = 632.8 nm. The presence of grafted primary amino groups was confirmed by reaction with fluorescein isothiocyanate (FITC, Research Organics) yielding a highly fluorescent product, accordingly to an in-house developed protocol. Fluorescence spectra of the different conjugated amino-functionalised microgel or nanogel were acquired with a JASCO FP-6500 spectrofluorimeter, equipped with a Xenon lamp (150 W).
Caspase 3 enzymatic assay on synthetic fluorescent substrate. MC3T3-E1 cells were seeded at high density on 6 well plate for 24 h in complete medium and grown for another 24 h after incubation with NGs. Cells were enzymatically detached from culture plate and extracted using a solution of Triton X 100 (1 %) in PBS. The amount of extracted proteins present in the

supernatant were quantified by Bradford micro assay method (Bio-Rad, Segrate, Milan, Italy) employing BSA (Sigma-Aldrich) as standard. MC3T3-E1 cells extracts (20µg), obtained as previously described, were used to detect the presence of activated caspases 3/7/8, typical apoptosis' marker. The Ac-Asp-Glu-Val-Asp-MCA peptide (Pepta Nova, Peptide Institute, inc), a specific substrate for activated caspase 3/7/8 was used. It ties a fluorophore in its cutting site, which emits fluorescence when cut by activated enzymes. In these experiments, the previously described extracts were added to 75 µL (8 µM) of the substrate in a 96 well plates. By spectrofluorimetric reading, it was possible quantify the degree of caspases activation. Spectrofluorimetric analysis were performed using Spectra Max Gemini EM-500 (Molecular Devices) and elaborated by Soft Max Pro 5.2 software.
MC3T3-E1 cell viability by MTT assay. The MC3T3-E1 cells were seeded in 96-well plate at density of 1x104 cell/well. After 24 h of growth in presences of NGs, cells were washed with PBS and then incubated with 200 µL/well of complete medium containing 0.25 mg/mL of MTT solution for 2 h at 37 C. After solubilisation of the resulting formazan product with 100µL/well of DMSO solution, the absorbance of intense purple staining at 490 nm wavelength was read on DU-730 Life Science Spectrophotometer (Beckman Coulter). MC3T3-E1 cells treated with DXR (5µM) for 24 h were used as positive control.

3. Results and discussion

It is well known that high dose-rate pulsed electron irradiation leads to either macrogels or nanogels depending on the polymer concentration in water. Irradiated aqueous solutions of a commercial PVP at concentrations ranging from above (from 10 %wt) to below (up to 0.05 %wt) its critical chain overlap concentration ($C^* \cong 1$ %wt (Dispenza et al., 2011)) were irradiated at a constant integrated dose (40 KGy) and dose rate (100 KGy/h). At a preliminary visual inspection, the irradiated samples from solutions at 10, 8 and 6 %wt appear completely macroscopically gelled, while at 4, 2 and 0.5 %wt present both macrogel islands and a separated aqueous phase. At lower concentrations, all irradiated systems appear optically transparent liquids, and they would "traditionally" classify as "sols", but DLS analysis revealed that liquids are actually NGs dispersions, as it will be discussed in the following. The yield of PVP crosslinking, either in the form of "infinite" networks or of "finite" nanoparticles, was always high (Dispenza et al., 2012). FTIR spectra of the dry networks have been compared to the linear, commercial PVP spectrum for macro-systems and NGs (spectra not presented here for sake of brevity). All the characteristic peaks of the linear PVP are also present in the macrogels spectra with no evident shifts, while spectra of nanogels show two new and well resolved peaks at 1769 and 1698 cm-1 near to the amide I band of the pyrrolidone ring: these peaks are generally associated to C=O (symmetric and asymmetric, respectively) stretching vibrations of 5-members cyclic imides. The appearance of the new band at 820 cm^{-1}, attributable to the ring CH_2 twisting of succinimide, further supports the aforementioned hypothesis that this new specie is formed. The crosslinked structures were also studied by CP/MAS solid state 13C-NMR spectroscopy that confirms the formation of the abovementioned specie.
Information about the effect of the polymer concentration on the particles size, the soluble part of the 0.5 %wt system and all the other systems produced at lower polymer concentration has been sought through DLS. Polymer concentration significantly influences the size of gel nanoparticles produced. In figure 1-A the calculated average Dh and relative standard deviations at the variance of polymer concentration are reported. The 0.5 and 0.25 %wt systems present nanoparticles with average Dh of 64 and 100 nm, respectively, that are higher than those of the not irradiated PVP coils. This can be due to the occurrence of both intermolecular and intramolecular crosslinking. On the contrary, NGs obtained from 0.1 and 0.05 %wt solutions have Dh lower than that of the corresponding not irradiated systems. In this case, intramolecular crosslinking may be the prevailing phenomenon. In order to completely rule out that chain-scission and molecular degradation phenomena are responsible for the reduction of Dh, a concomitant increase of light scattering intensity was observed with respect to the not-irradiated PVP aqueous solutions at the same concentration, that suggests an increment of

nanoparticles density. Dh changes also varying the average dose rate or the integrated dose when the polymer concentration in water is kept constant. In figure 1-B the effects of the average irradiation dose rate at the same integrated dose (40 kGy) for different polymer concentrations is shown, while in figure1-C the influence of the integrated dose (from 0 to 80 kGy) for two polymer concentrations (0.1 %wt and 0.25 %wt) is reported. The effect of increasing the average dose rate or the integrated dose on Dh goes in the same direction: when polymer aqueous solutions were irradiated under higher average dose rates or higher integrated doses, Dh increases and this effect is more pronounced for systems at higher polymer concentration. Average hydrodynamic diameters of amino-functionalised particles obtained by adding the functionalized monomer (APMAM) to the feedstock are reported in figure 1-D. Increasing APMAM content from 1:200 to 1:100 ratio, Dh only slightly increases, while at 50:1 ratio particle size step-wise rises to few microns, probably due to APMAM and/or APMAM oligomers bridging together many PVP chains. In order to understand this behavior it is necessary to emphasize that PVP can present both ionic and/or polar negative charges owing to keto-enolic tautomerisation of pyrrolidone carbonyls. Therefore, an APMAM molecule which is grafted to PVP, owing to the homolytic rupture of its unsaturated acrylic moiety, can also electrostatically interact with another PVP chain (or segment) with its terminal protonated amino group (pKa = 8.5).

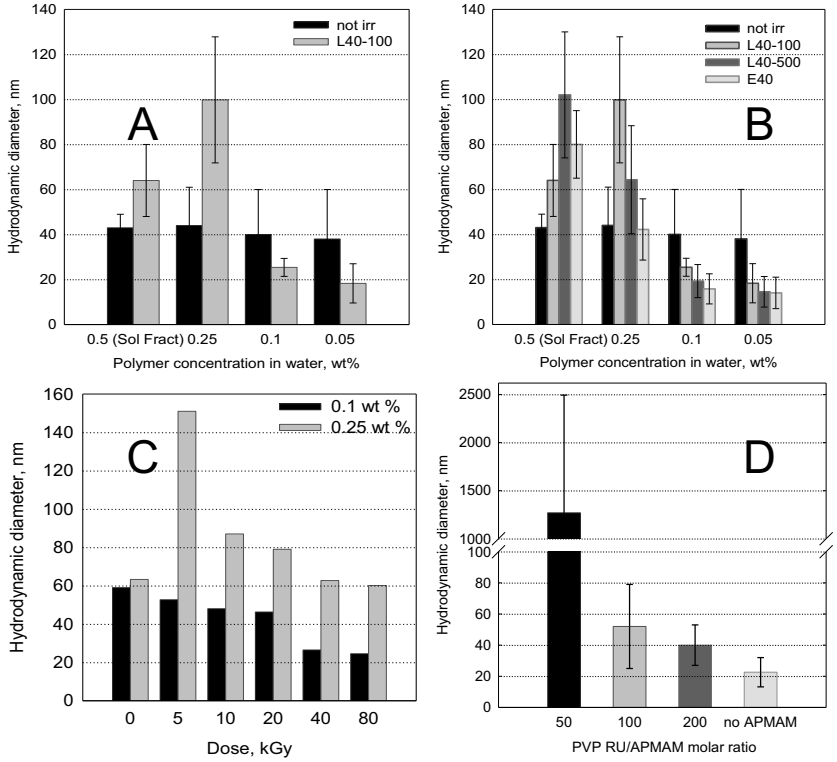

Figure 1: Average hydrodynamic diameters and relative standard deviation of solution of commercial PVP (K60) and irradiated PVP at the variance of the polymer concentrations (A); average dose rate for different polymer concentration (B); integrated dose for two polymer concentrations (C); APMAM molar ratio with respect to PVP RUs (D)

Chemical conjugation of fluorescein isothiocyanate (FITC) to the amino functionalized microgels and nanogels was attempted to explore whether the primary amines introduced with APMAM are available for chemoligation. Emission spectroscopy was used to assess the success of conjugation. In particular, Figure 3 shows the normalized emissions spectra of a typical PVP-

grafted-APMAM system conjugated with FITC (P*-g-A-FITC) in comparison with a buffered aqueous solution of the free probe at the same pH, a not-conjugated PVP-g-APMAM system (P*-g-A) and a base PVP nanogel dispersion, P*, that has been incubated with FITC according to the same protocol as for the amino-functionalized variants. Normalization allows easier identification of shifts in the maximum wavelength of emission. From the examination of this figure it is evident that the typical emission of a FITC-conjugated amino-grafted PVP micro/nanogel system is similar to that of the free probe but red shifted (+5 nm), which confirms the formation of thiourea bond. The base PVP nanogels incubated with FITC show a modest emission band, with a peak at an intermediate position between that of the free and the bound probe. This emission is likely caused by FITC physically entrapped in the gel particles. Conversely, all the conjugated P*-g-A systems show a distinct emission band at 520 nm, that suggest chemical attachment of FTIC.

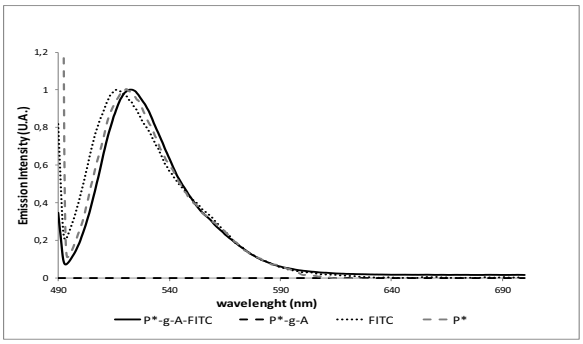

Figure 2: Normalized emissions of a typical FITC conjugated amino-grafted nanogel (microgel) formulation (λpeak=520 nm), of a FITC incubated base PVP formulation (λpeak=517 nm) and free FITC aqueous solution (λpeak=515 nm) all at the same pH (7.4 PBS).

A

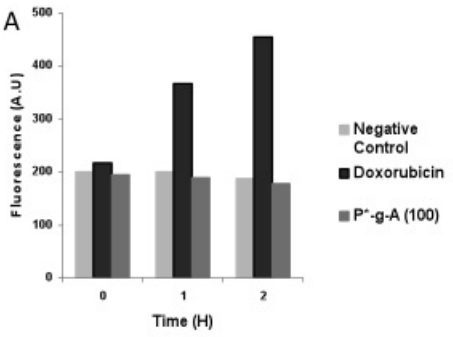

B

Samples	% of Living Cells
Negative Control	100±0,0036
Positive Control	70,79±0,0029
P*-g-A(100) 100µg	93,84±0,0043
P*-g-A(100) 50µg	94,53±0,0072
P*-g-A(100) 25µg	93,7±0,0038
P*-g-A(100) 12,5µg	87,90±0,0563

Figure 3: Biological evaluation of a typical amino-functionalized NG dispersion. A) Caspase 3 enzymatic assay on synthetic fluorescent substrate. B) MC3T3-E1 cell viability by MTT assay.

Biological evaluations in vitro were also performed to prove biocompatibility of NGs. MC3T3-E1 cells were incubated with P*-g-A (100) system and absence of cytotoxicity and cell viability were performed in order to assess if these nanoparticles influence cellular metabolism. Figure 3A shows MC3T3-E1 cells treated or not (negative control) with NGs at different times, compared to the ones treated with DXR (positive control). NG-treated cells did not show any activation of enzymes, while time-dependent fluorochrome release was observed in DXR-treated cells. In Figure 3B, MC3T3-E1 cells treated with different concentrations of NGs have similar profile to untreated cells; differently, DXR-treated cells (positive control) show a mortality of about 30 %. All gathered data suggest a good degree of biocompatibility of the produced NGs, they can be

considered suitable as nanocarriers in drug delivery applications or as building blocks for tissue-engineering scaffolds.

4. Conclusions

High energy radiation processing allows the production of biocompatible both base and amino-functionalised PVP NGs with high yields, no need of initiators, crosslinkers or recourse to toxic solvents and surfactants, therefore of complex purification procedures. Appropriate tuning of process parameters of industrial-type accelerators enables the control of the chemical structure and the size of the NGs produced, with adequate accuracy. Simultaneous sterilization can also be achieved, thus demonstrating the suitability of this technology for large scale production of NGs. Current developments are aimed at decorating these radiation-engineered nanogels with different biological moieties, such as complementary peptides, complementary antibody and enzyme fragments, to form bio-hybrid micro/nanoparticles with site-recognition functions or programmable hierarchical assembly.

References

Dispenza C., Ricca M., Lopresti C., Battaglia G., La Valle M., Giacomazza D., Bulone D., 2011, E-beam irradation and UV photocrosslinking of microemulsion-laden poly(N-vinyl-2-pyrrolidone) hydrogels for “in-situ” encapsulation of volatile hydrophobic compounds, Polym. Chem., 2 192-202.

Dispenza C., Grimaldi N., Sabatino M.A., Todaro S., Bulone D., Giacomazza D., Przybytniak G., Alessi S., Spadaro G., 2012. Studies of network organisation and dynamics of e-beam crosslinked PVPs: from macro to nano, Rad. Phys. Chem., DOI: 10.1016/j.radphyschem.2011.11.057.

Gonçalves C., Pereira P., Gama M., 2010, Self-Assembled Hydrogel Nanoparticles for Drug Delivery Applications, Materials, 3 1420-1460.

Lugao A.B., Malmonge S.M., 2001, Use of radiation in the production of hydrogels, Nucl. Instrum. Methods Phys. Res., Sect. B, 185, 37-42.

Morimoto N., Endo T., Iwasaki Y., Akiyoshi K., 2005, Design of hybrid hydrogels with self-assembled nanogels as cross-linkers: Interaction with proteins and chaperone-like activity, Biomacromolecules, 6, 1829-1834.

Muthu M.S., Feng S.S., 2010, Nanopharmacology of liposomes developed for cancer therapy, Nanomedicine, 5 (7) 1025.

Nishiyama N., 2007, Nanomedicine: Nanocarriers shape up for long life, Nature Nanotechnology, 2, 203.

Oh J.K., Drumright R., Siegwart D.J., Matyjaszewski K., 2008, The development of microgels/nanogels for drug delivery applications, Prog. Polym. Sci., 33, 448–477.

Peppas N.A., Hilt J.Z., Khademhosseini A., Langer R., 2006, Hydrogels in Biology and Medicine: From Molecular Principles to Bionanotechnology, Adv. Mater., 18, 1345–1360.

Rosiak J. M., Olejniczak J., 1993, Medical applications of radiation formed hydrogels, Rad. Phys. Chem., 42, 903-906.

Rosiak J.M., Ulanski P., Pajewski L.A., Yoshii F., Makuuchi K., 1995, Radiation formation of hydrogels for biomedical purposes. Some remarks and comments, Radiat. Phys. Chem., 46 161-168.

Rosiak J.M., Yoshii F., 1999, Hydrogels and their medical applications, Nucl. Instrum. Methods Phys. Res., Sect. B, 151, 56-64.

Sekhon B.S., Kamboj S.R., 2010, Inorganic nanomedicine—Part 2, Nanomedicine: Nanotechnology, Biology, And Medicine, 6, 612-618.

Shen M., Shi X., 2010, Dendrimer-based organic/inorganic hybrid nanoparticles in biomedical applications. Nanoscale, 2, 1596-1610.

Steinmetz N.F., 2010, Viral nanoparticles as platforms for next-generation therapeutics and imaging devices, Nanomedicine: Nanotechnology, Biology, And Medicine 6 634-641.

Ulanski P., Janik I. , Rosiak J.M, 1998. Radiation formation of polymeric nanogels, Radiat. Phys. Chem., 52, 289-294.